Neuromethods 153

Springer Protocols

Radek Pelc
Wolfgang Walz
J. Ronald Doucette *Editors*

Neurohistology and Imaging Techniques

MOREMEDIA

Humana Press

https://experiments.springernature.com/articles/10.1007/978-1-0716-0428-1_6

Chapter 6

Chemical Clearing of GFP-Expressing Neural Tissues

Klaus Becker, Saiedeh Saghafi, Christian Hahn, Nina Jährling, and Hans-Ulrich Dodt

Abstract

In the course of the recent rapid development of optical-sectioning and tomographic microscopy techniques, such as confocal microscopy, light-sheet microscopy, or optical coherence tomography (OCT), chemical tissue clearing experienced a renaissance. As most organic solvents commonly employed in tissue dehydration and clearing quench the green fluorescent protein (GFP) and related genetic markers, microscopy of chemically cleared GFP-expressing specimens remains a challenging task. In this chapter we review a variety of tissue-clearing methods and describe in detail a protocol that well preserves GFP fluorescence while maintaining tissue transparency.

Key words Light-sheet microscopy, Mouse brain, Hippocampus, Spinal cord, Tissue clearing, Dibenzyl ether, Tetrahydrofuran

Abbreviations

BABB	Benzyl alcohol/benzyl benzoate
BHT	Butyl hydroxytoluene
DBE	Dibenzyl ether
PBS	Phosphate-buffered saline
THF	Tetrahydrofuran

1 Introduction

1.1 Evolution of Chemical Tissue Clearing

The history of chemical clearing (or, to be more precise, optical clearing by chemical means) of biological preparations dates back to the beginning of the twentieth century when a German anatomist Werner Spalteholz published a pioneering study about this topic [1]. The clearing and brightening effect on biological tissues of some organic solvents and ethereal oils, such as Canada balsam, clove oil, carbon disulfide, and some other substances, was described even earlier, for example, by Lundvall [2, 3]. However,

Radek Pelc et al. (eds.), *Neurohistology and Imaging Techniques*, Neuromethods, vol. 153,
https://doi.org/10.1007/978-1-0716-0428-1_6,

Spalteholz was the first who investigated this effect systematically and understood the fundamental physical principle that matching the average refractive index of a sample to that of an incubation liquid soaking it markedly reduces light scattering generated by intra-tissue variations of the refractive index; consult Chapter 7 by Colarusso [4] for details. As a result, the specimens become translucent or even transparent, providing light absorption by any chromophores that may be present in them is only moderate [1, 5, 6]. Guided by this simple rule, Spalteholz tested various organic liquids, most of them ethereal oils, for their potential to optically clear organs isolated from humans and animals. In 1911 he published his results in German in a slim book entitled "On making human and animal specimens transparent" [1]. By screening various mixtures of organic solvents, largely composed of methyl salicylate, benzyl benzoate or isosafrole, Spalteholz found that a proportion of about 5:3 vol. parts of methyl salicylate/benzyl benzoate (or 3:1 vol. parts of methyl salicylate and isosafrole) is suitable for clearing of many anatomical preparations. This particular mixture became a standard for a commercial production of the so-called "Spalteholz preparations" by the Anatomical Institute of the Museum for Hygiene in Dresden, for which Spalteholz was occasionally working as a consultant.

Although Spalteholz's clearing method yielded high-grade anatomical demonstration samples sold to universities, anatomical institutions and schools worldwide, its scientific impact remained quite limited outside the anatomical education domain [7]. Distribution of these preparations had stopped in 1971 and Spalteholz's tissue-clearing technique slid into oblivion. In the following decades chemical tissue clearing was only rarely revisited, mainly in the field of embryology and developmental biology.

Owing to the rapid development of novel optical-sectioning and tomographic techniques allowing large fields of view and high depths of focus, such as optical projection tomography (OPT) [8], optical transmission tomography, optical emission tomography [9], and light-sheet microscopy [10–12] developed later on, chemical tissue clearing found new applications in deep-tissue imaging of large samples such as entire mouse brains or embryos [9, 10, 13–16].

Most clearing protocols are based on matching the refractive index of the immersion medium to that of the organic components of the tissue—typically the proteins. These solvents can be (a) lipophilic (non-polar) compounds easily penetrating the cell membranes or (b) hydrophilic (polar) substances composed of sugars, polyalcohols, or iodine compounds. In some cases the membrane permeability is enhanced by addition of detergents such as Triton X-100, sodium dodecyl sulfate (SDS), or saponin. While the first type (a) of clearing recipes requires a careful prior tissue dehydration, the second type (b) is directly applicable to fixed or unfixed tissues. Table 1 lists the chemical clearing techniques since 1897.

Table 1
A historical overview of chemical tissue-clearing techniques

Refs.	Author(s)	Dehydration medium	Clearing medium	Comments
[2, 3]	Lundvall 1904, 1905	Ethanol, benzene	Mixtures of benzene (mixed with peppermint oil) and carbon disulfide	Severely toxic vapors, very unpleasant smell of hydrogen sulfide
[1]	Spalteholz 1911	Ethanol, benzene	Mixtures of methyl salicylate with benzyl benzoate or isosafrole	Severe quenching of GFP fluorescence by methyl salicylate
[17]	Drahn 1922	Ethanol	Solutions of naphthalene in tetraline	Toxic vapors, intense smell of antimoth powder
[18]	Dent et al. 1989	Ethanol	"Murray's clear" 1:2 vol. parts of benzyl alcohol and benzyl benzoate (BABB)	Standard clearing medium for whole-mount preparations. Limited GFP compatibility
[19]	Chiang et al. 2002	None	Mixture of unknown composition, probably containing DMSO, diatrizoate acid, EDTA, glucamine, NADP, sodium diatrizoate and polyoxyalkalene derivatives	Distributed under the trade name FocusClear. High cost (~$180/5 mL), does not work in large specimens such as whole embryos or mouse brains
[20]	Staudt et al. 2007	None	2,2′-Thiodiethanol	Applicable to cultured cells, almost no clearing effect in tissues
[21]	Efimova and Anokhin 2009	2-Butoxy ethanol	75% Aqueous solution of sodium/meglumine diatrizoate	Specimens have to be dehydrated first; rehydration takes place in the clearing medium
[22]	Tsai et al. 2009	None	60% Sucrose solution, membrane permeabilization with 2% (v/v) Triton X-100	Transparency increase quite moderate, usable only in thin tissue slices
[23]	Hama et al. 2011	None	"Sca*l*eA2" 4M urea, 10% (w/v) glycerol and 0.1% (w/v) Triton X-100	Incubation time of several weeks, strong tissue swelling yielding high fragility
[13]	Ertürk et al. 2012	Tetrahydrofuran (THF), water- and peroxide-free	BABB (composition see above)	
[24]	Becker et al. 2012	Tetrahydrofuran (THF), water- and peroxide-free	Dibenzyl ether (DBE), water- and peroxide-free	

(continued)

Table 1
(continued)

Refs.	Author(s)	Dehydration medium	Clearing medium	Comments
[25]	Chung et al. 2013	None	Electrophoretic removal of cell membranes after embedding in polyacrylamide hydrogel for stabilization of morphological structures. Final clearing is achieved via incubation in FocusClear or glycerol	Owing to high permeability of cleared samples and excellent preservation of proteins molecular phenotyping and whole-mount immunostaining of cleared samples is possible

1.2 Solvent-Based (Lipophilic) Tissue Clearing with Benzyl Alcohol/Benzyl Benzoate (BABB)

To map the distribution of intermediate filament proteins during embryonic development, A. Murray developed a clearing medium consisting of a mixture of 1 vol part benzyl alcohol (BA) and 2 vol parts benzyl benzoate (BB), commonly abbreviated as BABB [18, 26]. Since BABB was found to be compatible with 4′,6-diamidino-2-phenylindole (DAPI) and other fluorescent markers, it became a standard tissue-clearing medium for deep-tissue imaging of whole-mount preparations in embryological research. Compared to methyl salicylate which also found a widespread use as a tissue-clearing medium [27], BABB generally provides better and faster clearing results even though its refractive index (~1.56) is very close to that of methyl salicylate (~1.54). BABB's much lower polarity (water solubility 0.0154 g/L vs. ~0.7 g/L for methyl salicylate) enabling better penetration through cell membranes, lipidic (non-polar) in nature is the most likely explanation. Unfortunately, BABB significantly quenches the fluorescence of GFP over time. Therefore, to achieve sufficiently high fluorescence intensities, incubation times should be kept as short as possible [10]. Furthermore, high GFP-expression rates are required. Recently, it was demonstrated that substitution of BABB with dibenzyl ether (DBE) yields superior GFP fluorescence and better tissue transparency [24]. A DBE-based, GFP-friendly dehydration and clearing protocol for large samples such as mouse brains or entire embryos is described in Subheading 1.4.

1.3 Water-Based (Hydrophilic) Tissue-Clearing Reagents

In recent years various attempts have been made to develop water-based clearing media inherently not requiring tissue dehydration and applicable to both fixed and unfixed specimens.

CellExplorer Labs (Taiwan) distribute a water-miscible tissue-clearing medium with a brand name FocusClear containing dimethyl sulfoxide (DMSO), diatrizoate acid, EDTA, glucamine, NADP, sodium diatrizoate and polyoxyalkalenes in unspecified proportions [19] FocusClear has a refractive index of 1.45 and was successfully applied to clear, for example, insect brains [28]

and murine intestine [29]. Its price of about $180/5 mL vial makes it significantly more expensive than custom-made clearing media, thereby limiting its use to small samples such as tissue slices. FocusClear preserves fluorescence of GFP and related markers [30, 31] but poorly penetrates lipid-rich myelinated tissue.

Staudt el al. [20] introduced 2,2′-thiodiethanol (TDE) as another hydrophilic mounting medium for cultured cells. Its refractive index of ~1.52 can be adjusted by dilution with water ($n = 1.33$) in any proportion. Due to its very low penetration rate it cannot be used in large objects such as whole-mount preparations. While TDE can partly quench GFP fluorescence the fluorescence of some other markers such as Cy3 can even be amplified [20].

In a similar approach, Efimova and Anokhin [21] used a customized ~75% aqueous mixture of sodium diatrizoate and meglumine diatrizoate to clear entire mouse brains. Due to the high content of iodine (a heavy element) diatrizoic acid exhibits high X-ray opacity. Its salts are thus used as contrast agents for intestinal medical radiography and are commercially available, for example, under the trade names Hypaque 76% (Amersham Health, USA), and Gastrografin or Urografin (Bayer, Germany). These products contain meglumine diatrizoate and sodium diatrizoate in varying proportions, and all have a high refractive index of about 1.45. However, due to high polarity, their penetration through the cell membranes is very slow in nondehydrated tissues. Efimova and Anokhin [21] circumvented this problem by a prior dehydration of mouse brains in an ascending concentration row of 2-butoxy ethanol. While dehydration may accelerate the diffusion of diatrizoate solutions into the tissue by permeabilizing cell membranes, potential advantages of a water-based tissue-clearing medium such as the elimination of dehydration-induced shrinking artifacts and some gain of time do not seem to outweigh the drawbacks.

Tsai et al. [22] cleared murine brain slices in 60% aqueous solutions of sucrose, after permeabilizing the cell membranes using the detergent Triton X-100. While the clearing effect may be sufficient in some applications, the increase of tissue transparency that can be achieved is quite modest, so that only thin samples such as brain slices can be processed. Although not tested yet we do not expect the described procedure to have any major effect on the fluorescence of GFP and other genetic markers.

Recently, Hama et al. [23] presented "Sca*l*e," an aqueous solution consisting of urea, glycerol and a small addition of the detergent Triton X-100, as a clearing medium. Hama et al. suggest different variations of this solution, named Sca*l*eA2, Sca*l*eU2, and Sca*l*eB4. Sca*l*eA2 contains 4M urea and 10% (w/v) glycerol and 0.1% (w/v) Triton X-100; Sca*l*eU2 contains 4M urea, 30% (w/v) glycerol, and 0.1% (w/v) Triton X-100; and Sca*l*eB4 contains 8M urea and 0.1% (w/v) Triton X-100. The pH of Sca*l*eB4 was

adjusted to 8.7 [23]. Presently, Sca*l*eA2 is distributed by Olympus under the brand name "Scaleview-A2", jointly with specialized long working distance (WD) immersion objectives (×25/1.0 at WD 4 mm; ×25/0.90 at WD 8 mm). These are corrected for the refractive index of Sca*l*eA2 (~1.38). In contrast to most other clearing liquids causing tissue shrinkage and hardening, specimens cleared with Sca*l*e exhibit pronounced swelling, up to double the original volume. According to Hama et al. [23], their clearing procedure does not show any appreciable quenching effect on the fluorescence of EGFP and other fluorescent proteins (mAG1, YFP, DsRed, and mCherry) while it is inevitable at least to a certain degree when nonpolar solvents such as BABB or DBE are used.

Samples cleared with Sca*l*eA2 generally exhibit a soft and fragile texture so that they have to be handled very carefully; this problem can be solved by switching to one of the other two variants (Sca*l*eU2 or Sca*l*eB4) [23]. At 656 nm, the refractive index of Sca*l*eA2 is 1.38, which is much lower compared to other tissue-clearing media designed to match the refractive index of proteins (~1.53). This implies that the clearing effect of Scaleview does not rely on refractive-index matching but presumably on structural modifications of proteins such as collagen [5] and the pronounced tissue-swelling effect due to the absorption of water. As with all other aqueous solutions, clearing with Sca*l*e requires long incubation times, for example, about 2 weeks for E13.5 (13.5-day-old) mouse embryo. Generally, for Sca*l*eA2 and Sca*l*eU2 the authors report incubation times in the order of days/weeks and weeks/months, respectively [23].

While Sca*l*e may sufficiently clear E13.5 mouse embryos and very young mouse brains below P14 (postnatal day 14), it does not clear highly myelinated regions. In our experiments, poor or even no clearing was obtained in large or fatty specimens, such as nervous tissue with all variations of Sca*l*e. This is not surprising as myelin layers consist of a fatty substance and can thus only be penetrated by lipophilic solvents. We failed to clear muscle samples of about 5–10 mm edge length by incubation in Sca*l*eA2, Sca*l*eU2 or Sca*l*eB4 or for about 10 weeks [24]. After this time span the specimen clearly began to show signs of structural decomposition.

At first, water-based tissue-clearing media appear promising as they do not require prior specimen dehydration, thus preventing possible shrinking artefacts. However, as long incubation times are needed there is generally no gain in the clearing rate compared to the procedures involving dehydration. To our knowledge, there is currently no alternative to nonpolar organic solvents when clearing heavily myelinated or fatty samples (e.g., entire mouse brains or human tumor biopsies of ~10 mm edge length).

However, this situation may change owing to a novel clearing approach presented in 2013 by Chung et al. [25]. In their method referred to as "CLARITY" the specimen morphology is well

preserved in a first step by perfusion with a mixture of acrylamide, bisacrylamide, and formaldehyde that can be thermally polymerized to an elastic hydrogel. By incubation at 37 °C the monomers are further cross-linked to proteins, nucleic acids and some other small, low molecular weight cellular compounds, thus forming a hybrid, mechanically stable molecular mesh.

Since lipids are not integrated into the hydrogel mesh, they can be extracted from the sample via a modified form of SDS-PAGE electrophoresis in a second step. The polymerized molecular mesh preserves the biomolecules and fine structural features such as membrane-localized proteins, synapses and spines, thus preventing their displacement during this extraction procedure. After lipid extraction the specimens are incubated for some time in an aqueous clearing medium such as FocusClear (CellExplorer Labs, Taiwan), or 80% glycerol to preserve their final transparency [25].

Chung et al. [25] have also achieved an excellent conformational preservation of functional proteins and a high permeability for aqueous solutions, making the cleared samples accessible to molecular phenotyping as well as whole-mount immunostaining, which is not possible with other clearing techniques described before.

1.4 Chemical Clearing of GFP-Expressing Tissues with Tetrahydrofuran and Dibenzyl Ether

Generation of GFP-expressing transgenic animals enables histological studies of neuronal networks with unprecedented accuracy [32]. Therefore, GFP became one of the most common genetic reporters in molecular biology, medicine and cell biology. However, GFP is of limited compatibility with common dehydration and tissue-clearing techniques. For example, ethanol and BABB as frequently used tissue-dehydration and clearing media considerably quench the fluorescence of GFP and related markers. This is a severe drawback which can turn clearing, staining and embedding of GFP-expressing material into a rather difficult task [33].

To overcome this problem we systematically screened potential dehydration and clearing media (Table 2) and demonstrated in GFP-labeled mouse brains and spinal cords that dehydration with tetrahydrofuran (THF) yields stronger fluorescence with a markedly reduced background [13, 24]. We also found that clearing with dibenzyl ether (DBE, Fig. 1B) better preserves fluorescence and achieves higher tissue transparency [24]. Combined, dehydration with THF and clearing with DBE is well suited to GFP-expressing specimens and is applicable to mouse spinal cords, entire mouse embryos, entire *Drosophila* and other specimens; mouse hippocampi are shown in Fig. 2. Since THF and DBE are chemically inert ethers, it may be speculated that it is this chemical quality that is responsible for their good GFP compatibility.

Tissue shrinking is an unavoidable side-effect of any dehydration procedure and is slightly higher in THF than in ethanol. However, this shrinkage is the same (about 20%) in each direction (i.e., isotropic) for murine spinal cord [24] and the shrinking artifacts we observed were no greater than in ethanol. The contribution of the clearing medium (BABB or DBE) to the total tissue shrinkage is negligible [13, 24].

Clearing with DBE proceeds faster than with BABB. This is likely due to the lower viscosity of DBE translating to faster tissue penetration. Compared to the dynamic viscosities of benzyl alcohol and benzyl benzoate (6.4 cP and 10 cP, respectively) the viscosity of DBE (5.3 cP) is rather low.

An additional benefit of DBE over BABB is its lower toxicity. Indeed, it is used as a stabilizer in perfumes and as a food-flavoring agent. In rats no toxic effects of a 196 mg/kg/day dose of DBE were found [35]. Furthermore, DBE (~$40/L) is considerably cheaper than BABB (BA ~$300/L, BB ~$100/L).

Table 2
Dehydration and clearing chemicals tested

Dehydration	
Dehydration medium	**GFP fluorescence after clearing with BABB[a]**
 Methanol	Severely reduced
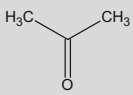 Acetone	Not detectable
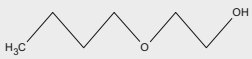 2-butoxyethanol	Severely reduced
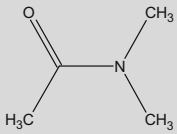 Dimethyl formamide	Severely reduced
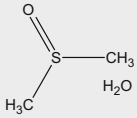 Dimethyl sulfoxide (DMSO)	Severely reduced
 Dioxane	Severely reduced
 Tetrahydrofuran	**Well preserved**

Clearing		
Clearing medium	***n*[b]**	**Clearing efficiency and GFP fluorescence after ethanol dehydration**
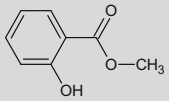 Methyl salicylate	1.54	Poor clearing, fluorescence strongly reduced
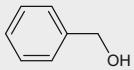 Benzyl alcohol	1.54	Poor clearing, fluorescence reduced
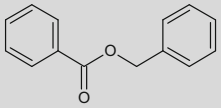 Benzyl benzoate	1.57	Poor clearing, fluorescence reduced
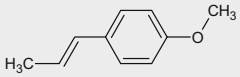 Trans-anethole	1.56	Good clearing and preservation of fluorescence; brownish discolorations
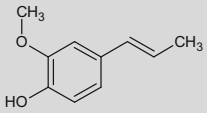 Isoeugenol	1.58	Good clearing and preservation of fluorescence; strong brownish discolorations
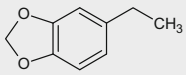 Isosafrole	1.57	Poor clearing, fluorescence strongly reduced
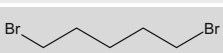 1,5-bromopentane	1.51	No clearing at all
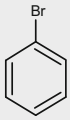 Bromobenzene	1.56	Good clearing and preservation of fluorescence; significant toxicity and high volatility
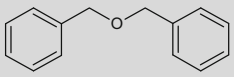 Dibenzyl ether	1.56	**Good clearing and preservation of fluorescence**

Most of the substances found to be GFP-incompatible possess hydroxyl or carbonyl groups. Adapted from Ref. [24]
[a]Benzyl alcohol/benzyl benzoate
[b]Refractive index (rounded to 0.01)

2 Preparation of Chemical Agents

THF as well as DBE can become contaminated with peroxides over time due to contact with oxygen [24]. After long-term storage, DBE can additionally become contaminated with benzaldehyde [36] (Fig. 3). Since both of these substances quench GFP fluorescence even at low concentrations, THF and DBE should always be purified before use by column chromatography and stored in brown glass bottles containing a molecular sieve of 3 Å pore as a protection from water, and access of oxygen prevented by covering the liquid with argon as an inert gas.

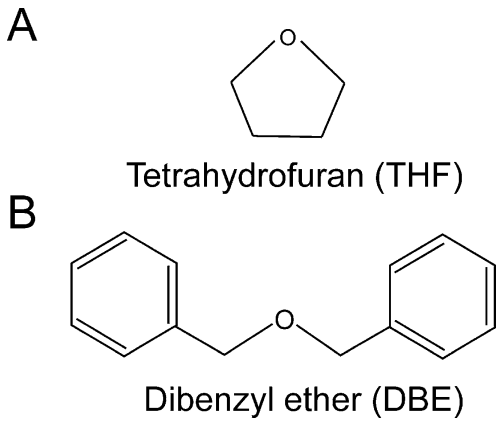

Fig. 1 Chemical structures of tetrahydrofuran and dibenzyl ether. Interestingly, both compounds are ethers lacking any functional groups

2.1 Tetrahydrofuran and Dichloromethane

Peroxide removal from THF was carried out by column absorption chromatography (Fig. 4A) with basic activated aluminum oxide, ca. 250 g/L) [24, 37]. However, chromatography also removes the stabilizer BHT normally present in commercially available THF. For safety reasons, generation of dangerous amounts of peroxides due to exposure to sunlight or oxygen must be prevented by replacing BHT after chromatography, for example, by adding 250 mg/L into the receiver flask (Fig. 4A-*3*) protected from light by an aluminum foil. Insufficiently stabilized THF can explode with fatal consequences! Peroxide concentrations were estimated using Quantofix test stripes.

Chemicals

- Tetrahydrofuran (THF, Sigma-Aldrich 186562).
- Aluminum oxide (basic-activated Brockmann I grade, Sigma-Aldrich 199443).
- Butylhydroxytoluene (BHT, Sigma-Aldrich W218405).
- Calcium chloride (Sigma-Aldrich C1016).
- Dichloromethane (Carl Roth, Germany, 7334).
- Quantofix Peroxide 25 test stripes (Sigma-Aldrich Z249254).
- Argon gas.

Equipment

- Brown-glass storage bottle.
- Dropping funnel with pressure compensation (Fig. 4A-*1*).
- Chromatography column (Fig. 4A-*2*).
- Two-necked round bottom flask (Fig. 4A-*3*) wrapped in aluminum foil.
- Drying tube filled with calcium chloride (Fig. 4A-*4*).
- Rubber and glass joints.
- Silicon tubes (2×).

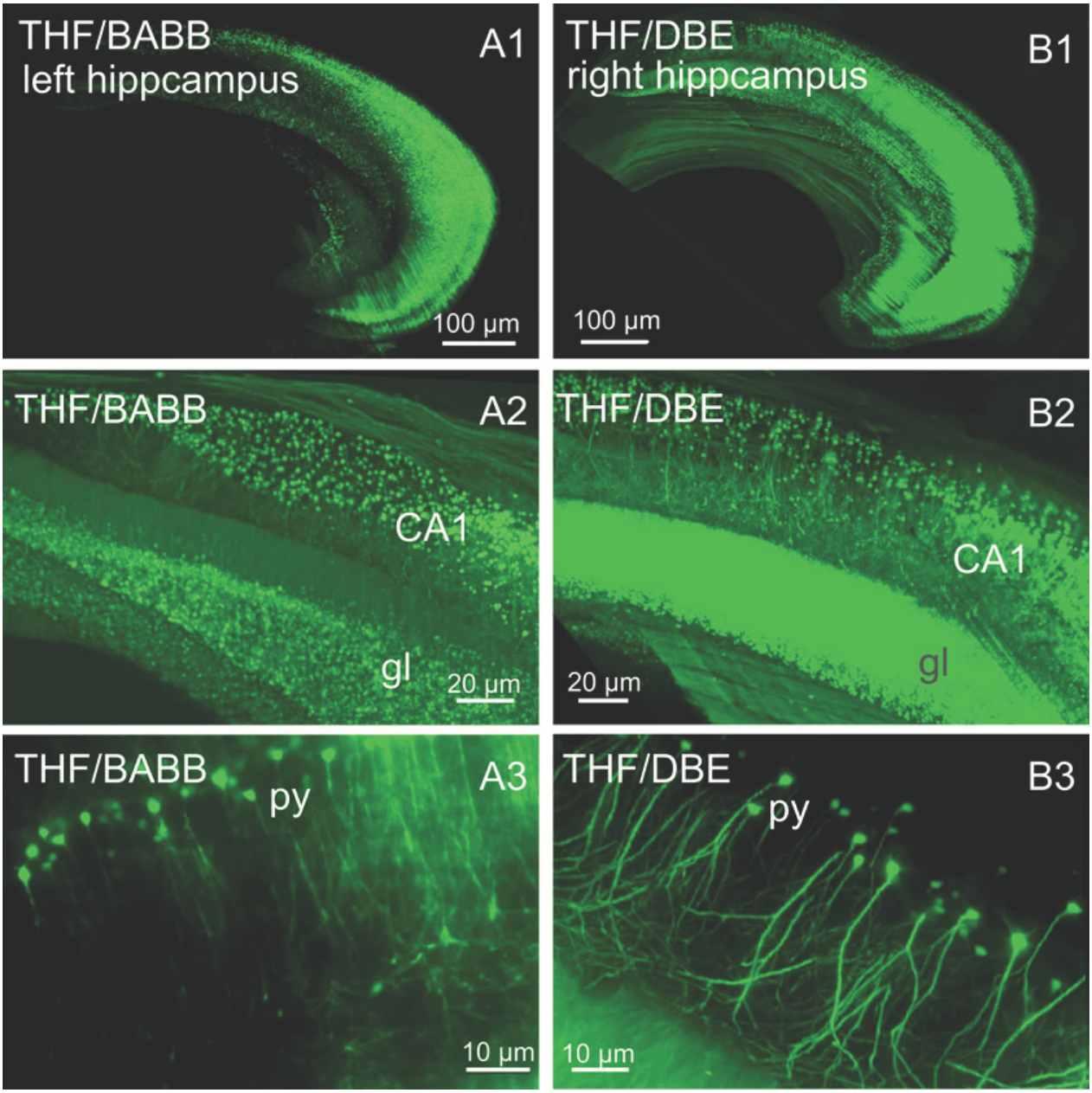

Fig. 2 Ultramicroscopy-based reconstructions of isolated hippocampi from thy-1 EGFP-M mouse. Dibenzylether (DBE) clearing yields stronger fluorescence and better visibility of details. (**A1**–**A3**) Left hippocampus dehydrated with tetrahydrofuran (THF) and cleared with benzyl alcohol/benzyl benzoate (BABB). (**B1**–**B3**) Right hippocampus (from the same mouse) dehydrated with THF and cleared with DBE. *CA1* *cornu ammonis* region one, *gl* granular cell layer, *py* pyramidal cells. All images were acquired with an Olympus objective XLFluor 4×/0.28 and an imaging setup described earlier [10, 13, 15] and in Chapter 11 by Saghafi [34]. Adapted from Ref. [24]

2.2 Dibenzyl Ether

Compared to THF, DBE's viscosity and boiling point are higher, so the removal of its peroxides was carried out using a different setup (Fig. 4B). The filter funnel was filled with ~250 g of activated aluminum oxide per liter, and suction was applied to the receiver flask [24]. Peroxide concentrations were estimated using Quantofix test stripes. The presence of unwanted aldehydes (such as benzaldehyde, Fig. 3) and ketones was checked by applying Brady's test

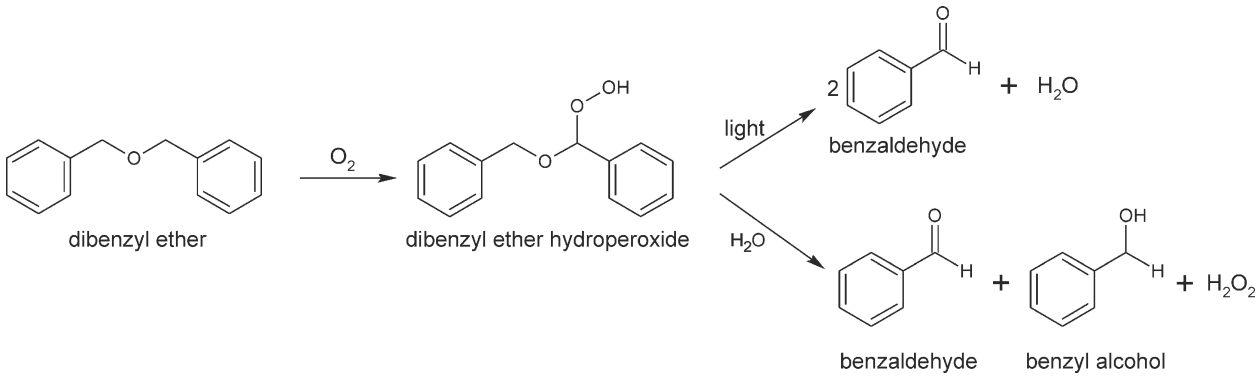

Fig. 3 Chemical decomposition of dibenzyl ether (DBE) by oxygen. Oxygen can transform dibenzyl ether into an instable peroxide, which then further reacts, yielding benzaldehyde and benzyl alcohol

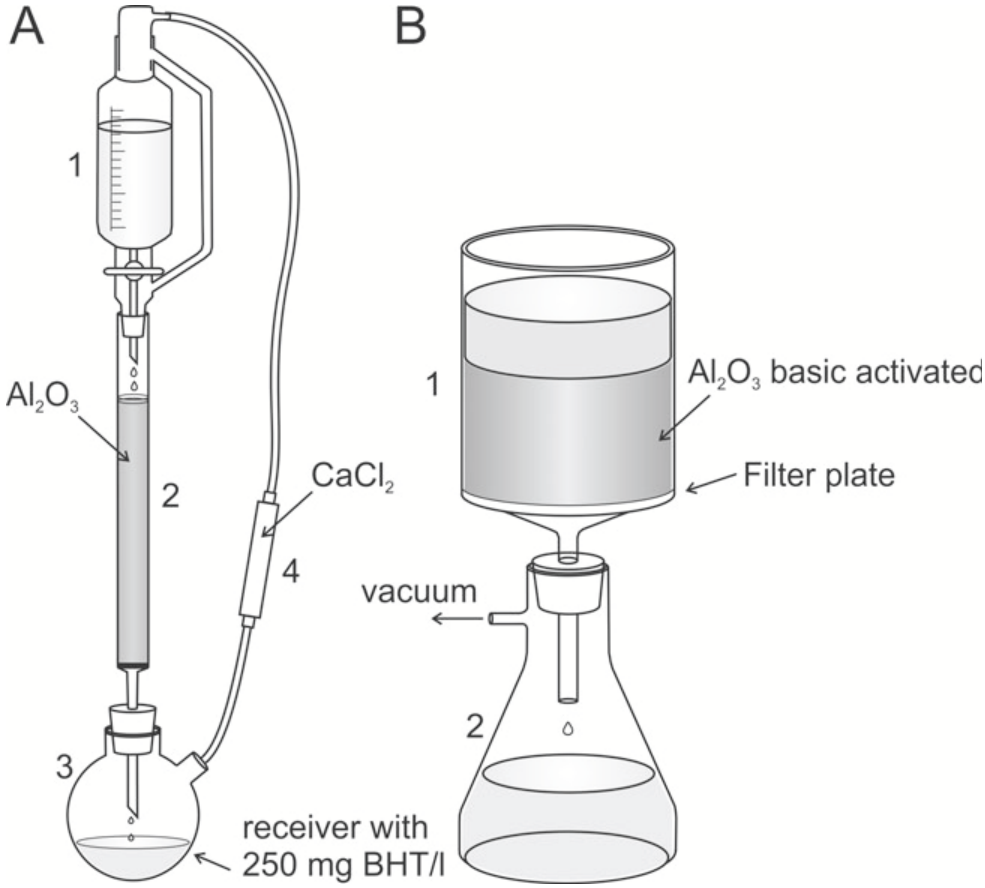

Fig. 4 Peroxide removal apparatus. (**A**) Peroxide removal from tetrahydrofuran (THF) and dichloromethane. (*1*) Dropping funnel with pressure compensation. (*2*) Chromatography column filled with basic-activated aluminum oxide. (*3*) Two-necked round-bottom flask filled with butylhydroxytoluene (BHT) as a stabilizer of THF. (*4*) Drying tube filled with calcium chloride. (**B**) Peroxide removal from dibenzyl ether and benzyl alcohol/benzyl benzoate. (*1*) Filter unit with a filter plate (16–40 μm pore size). (*2*) Vacuum-tight filtering flask. Reprinted from Ref. [24]

[38]. Chemically, the amino group of 2,4-dinitrophenylhydrazine (Brady's reagent) reacts with them by addition-elimination of carbonyl groups, yielding insoluble hydrazine manifesting itself as an orange precipitate.

Chemicals

- Aluminum oxide (basic-activated Brockmann I grade, Sigma-Aldrich 199443).
- Dibenzyl ether (DBE, Sigma-Aldrich 108014).
- Molecular sieve (3 Å mesh, Sigma-Aldrich 208582).
- Quantofix Peroxide 25 test stripes (Sigma-Aldrich Z249254).
- Brady's Reagent (2,4-dinitrophenylhydrazine, Sigma-Aldrich D199303; 4 g dissolved in 8 mL of concentrated sulfuric acid, 90 mL of methanol and 10 mL of water).

Equipment

- Brown-glass storage bottle.
- Büchner funnel with filter plate of 16–40 μm pore width (Fig. 4B-*1*).
- Vacuum-tight filtering flask (Fig. 4B-*2*).
- Silicon tubes and joints.
- Vacuum pump LABOPORT (KNF, USA).

2.3 Formaldehyde/PBS

For 1 liter of fixative 40 g of paraformaldehyde powder (a solid polymer of formaldehyde) was added and dissolved in phosphate-buffered saline (PBS) at 60 °C while stirring; a slightly basic pH (NaOH) is required. Since GFP fluorescence is stabilized under basic conditions, pH was adjusted to 7.8. Formaldehyde solution (4%) was kept at 4 °C and only stored for a few days. Please consult Chapter 2 by Mufson [39] for properties of paraformaldehyde.

Chemicals

- Deionized water.
- Paraformaldehyde (Sigma-Aldrich 6148).
- PBS 10 mM (Dulbecco, Biochrom AG, Germany L182).
- Sodium hydroxide (NaOH).

3 Perfusion of Mice and Dissection of Neural Tissues

14 days old thy-1 EGFP-M (c57/bl6) mice [40] were killed by asphyxiation in CO_2, transcardially perfused *post mortem* with at least 20 mL of PBS (pH 7.8) containing 10 Units/mL of heparin until blood was removed, and perfusion-fixed by 100 mL of 4% formaldehyde in PBS (pH 7.8), as follows: The mouse (with its head pointing away from the experimentalist) was pinned ventral-

side-up onto the dissection plate and its ventral part moistened with ethanol. Its abdominal wall and chest were opened, a perfusion cannula carefully inserted into the left heart ventricle and fixed with a microvascular clamp. Finally, the right heart auricle was opened with small scissors. The flexible tube of the cannula was clamped in a peristaltic pump. The mouse should only be perfused slowly (1.5–2.0 mL/min) with PBS and formaldehyde (both on ice). No major blood vessels, lung or liver should be hurt during the dissection.

After perfusion the brain was removed from the skull and post-fixed in 4% formaldehyde/PBS (pH 7.8 at 4 °C) overnight. Next day, the specimens were rinsed 3× in PBS (at room temperature, 30 min each) and immediately dehydrated. Animal care and euthanasia were carried out in accordance with the local ethic guidelines and animal protection laws.

Hippocampi were dissected from the brain by splitting it into hemispheres, detached by dilation of the flanking ventricles using Dumont #5 forceps, and post-fixed overnight in 4% formaldehyde/PBS (pH 7.8), rinsed 3× in PBS (15 min each), and immediately dehydrated.

Spinal cord was dissected by removing the viscera and cutting the vertebral column, for example, above the lumbar vertebrae by using appropriate scissors. The vertebral column was carefully cut out and the spinal cord taken out by cutting the spinal nerves using Dumont #5 forceps and spring scissors. Spinal cords were processed in the same way as hippocampi.

Chemicals/Equipment

- Heparin (Sigma-Aldrich, Germany).
- Carbon dioxide supply and an asphyxiation chamber.
- Butterfly cannula (Nipro 21G, with a flexible tube).
- Microvascular clamp (S&T, Switzerland, P-3, 70007).
- Peristaltic pump (Ismatec ISM796B).
- Spring scissors (Fine Science Tools, 15006-09, 10 mm bladed angled side).
- Standard dissection equipment (small scissors for opening the mouse, larger scissors for decapitation, dissection plate with pins, forceps for handling, appropriate spatula for removing the brain from the skull).

4 Tissue Dehydration and Clearing

Dehydration and clearing of the dissected neural tissues was carried out at room temperature under an extraction hood in 15 mL glass

vials filled with ca. 10 mL of dehydration/clearing solution and fitted with a tight lid. A rotary mixer was employed to facilitate penetration of the solution into the samples.

4.1 Dehydration

The fixed brains were dehydrated as a whole or split into hemispheres. To minimize shrinkage of brain, hippocampi, and spinal cord, water was removed by incubating in an ascending concentration row of water-diluted or pure peroxide-free THF, as outlined below. For spinal cord, we additionally recommend a 1-h incubation step in dichloromethane after dehydration, to remove myelin and facilitate subsequent clearing.

- Brain: 50, 70, 80, 96 vol.%, finally 3× pure agent (100%), 12 h/step.
- Hippocampi: 50, 80, 96 vol.%, finally 3× 100%, 1 h/step, last step overnight.
- Spinal cord: 50, 80, 96 vol.%, finally 3× 100%, 1 h/step, last step overnight.

4.2 Clearing

Clearing of the dehydrated specimens was carried out in peroxide-free DBE until becoming transparent, as outlined below:

- Brain: 1–2 days, three exchanges of clearing medium.
- Hippocampi: ca. 1 day, two exchanges of clearing medium.
- Spinal cord: ca. 1 day, one exchange of clearing medium.

References

1. Spalteholz W (1911) Über das Durchsichtigmachen von menschlichen und tierischen Präparaten. S. Hirzel, Leipzig. http://s2w.hbz-nrw.de/zbmed/content/titleinfo/555354
2. Lundvall H (1904) Über demonstration embryonaler Knorpelskelette. Anatomischer Anzeiger (Jena) 25:219–222. BHL: 11889861. https://biodiversitylibrary.org/page/11889861
3. Lundvall H (1905) Weiteres über demonstration embryonaler Skelette. Anatomischer Anzeiger (Jena) 27:520–523. BHL: 11893322. https://biodiversitylibrary.org/page/11893322
4. Colaruso P (2020) The properties of light governing biological microscopy. In: Pelc R, Walz W, Doucette JR (eds) Neurohistology and imaging techniques, Neuromethods, vol 153. Springer (Humana Press), New York, pp 201–223. https://doi.org/10.1007/978-1-0716-0428-1_7
5. Rylander G, Stumpp OF, Milner TE, Kemp NJ, Mendenhall JM, Diller KR, Welch AJ (2006) Dehydration mechanism of optical clearing in tissue. J Biomed Opt 11 (4):041117. https://doi.org/10.1117/1.2343208
6. Tuchin VV (2005) Optical clearing of tissues and blood. SPIE Press, Bellingham (WA, USA). ISBN: 9780819460066
7. Keller PJ, Dodt H-U (2011) Light sheet microscopy of living or cleared specimens. Curr Opin Neurobiol 22(1):1–6. https://doi.org/10.1016/j.conb.2011.08.003
8. Sharpe J, Ahlgreen U, Perry P, Hill B, Ross A, Hecksher-Sorensen J, Baldock R, Davidson D (2002) Optical projection tomography as a tool for 3D microscopy and gene expression

studies. Science 296(5567):541–545. https://doi.org/10.1126/science.1068206

9. Oldham M, Sakhalkar H, Oliver T, Allan JG, Dewhirst M (2008) Optical clearing of unsectioned specimens for three-dimensional imaging via optical transmission and emission tomography. J Biomed Opt 13(2):021113. https://doi.org/10.1117/1.2907968
10. Dodt H-U, Leischner U, Schierloh A, Jährling N, Mauch CP, Deininger K, Deussing JM, Eder M, Zieglgänsberger W, Becker K (2007) Ultramicroscopy: three-dimensional visualization of neuronal networks in the whole mouse brain. Nat Methods 4 (4):331–336. https://doi.org/10.1038/nmeth1036
11. Huisken J, Swoger J, Del Bene F, Wittbrodt J, Stelzer EH (2004) Optical sectioning deep inside live embryos by selective plane illumination microscopy. Science 305 (5686):1007–1009. https://doi.org/10.1126/science.1100035
12. Voie AH, Burns DH, Spelman FA (1993) Orthogonal-plane fluorescence optical sectioning: three-dimensional imaging of macroscopic biological specimens. J Microsc 170 (Pt3):229–236. https://doi.org/10.1111/j.1365-2818.1993.tb03346.x
13. Ertürk A, Becker K, Jährling N, Mauch CP, Hojer CD, Egen JG, Hellal F, Bradke F, Sheng M, Dodt H-U (2012) Three-dimensional imaging of solvent-cleared organs using 3DISCO. Nat Protoc 7(11):1983–1995. https://doi.org/10.1038/nprot.2012.119
14. Jährling N, Becker K, Schönbauer C, Schnorrer F, Dodt H-U (2010) Three-dimensional reconstruction and segmentation of intact Drosophila by ultramicroscopy. Front Syst Neurosci 4(1):1–6. https://doi.org/10.3389/neuro.06.001.2010
15. Becker K, Jährling N, Kramer ER, Schnorrer F, Dodt HU (2008) Ultramicroscopy: 3D reconstruction of large microscopical specimens. J Biophotonics 1(1):36–42. https://doi.org/10.1002/jbio.200710011
16. Sakhalkar HS, Dewhirst M, Oliver T, Cao Y, Oldham M (2007) Functional imaging in bulk tissue specimens using optical emission tomography: fluorescence preservation during optical clearing. Phys Med Biol 52(8):2035–2054. https://doi.org/10.1088/0031-9155/52/8/001
17. Drahn F (1922) Ein neues Durchtränkungsmittel für histologische und anatomische Objekte. Berl Tierarztl Wochenschr 38:97–100
18. Dent JA, Polson AG, Klymkowsky MW (1989) A whole-mount immunocytochemical analysis of the expression of the intermediate filament protein vimentin in *Xenopus*. Development 105(1):61–74. PMID: 2806118. https://www.ncbi.nlm.nih.gov/pubmed/2806118
19. Chiang AS (2002) Aqueous tissue clearing solution. Patent US6472216B1. https://patents.google.com/patent/US6472216B1
20. Staudt T, Lang MC, Medda R, Engelhardt J, Hell S (2007) 2,2'-Thiodiethanol: a new water soluble mounting medium for high resolution optical microscopy. Microsc Res Tech 70 (1):1–9. https://doi.org/10.1002/jemt.20396
21. Efimova OI, Anokhin KV (2009) Enhancement of optical transmission capacity of isolated structures in the brain of mature mice. Bull Exp Biol Med 147(1):3–6. https://doi.org/10.1007/s10517-009-0463-9
22. Tsai PS, Kaufhold JP, Blinder P, Friedman B, Drew PJ, Karten HJ, Lyden PD, Kleinfeld D (2009) Correlations of neuronal and microvascular densities in murine cortex revealed by direct counting and colocalization of nuclei and vessels. J Neurosci 29(46):14553–14570. https://doi.org/10.1523/JNEUROSCI.3287-09.2009
23. Hama H, Kurokawa H, Kawano H, Ando R, Shimogori T, Noda H, Fukami K, Sakaue-Sawano A, Miyawaki A (2011) Sca*l*e: a chemical approach for fluorescence imaging and reconstruction of transparent mouse brain. Nat Neurosci 14(11):1481–1488. https://doi.org/10.1038/nn.2928
24. Becker K, Jährling N, Saghafi S, Weiler R, Dodt H-U (2012) Chemical clearing and dehydration of GFP expressing mouse brains. PLoS One 7(3):e33916. https://doi.org/10.1371/journal.pone.0033916
25. Chung K, Wallace J, Kim SY, Kalyanasundaram S, Andalman AS, Davidson TJ, Mirzabekov JJ, Zalocusky KA, Mattis J, Denisin AK, Pak S, Bernstein H, Ramakrishnan C, Grosenick L, Deisseroth K (2013) Structural and molecular interrogation of intact biological systems. Nature 497 (7449):332–337. https://doi.org/10.1038/nature12107
26. Klymkowsky MW, Hanken J (1991) Whole-mount staining of Xenopus and other vertebrates. In: Kay BK, Peng HB (eds) *Xenopus laevis*: practical uses in cell and molecular biology, Meth Cell Biol, vol 36. Academic Press, New York, pp 419–441. https://doi.org/10.1016/S0091-679X(08)60290-3
27. Skinner RA (1986) The value of methyl salicylate as a clearing agent. J Histotechnol 9 (1):27–28. https://doi.org/10.1179/his.1986.9.1.27

28. Chiang AS, Liu YC, Chiu Sl HSH, Huang CY, Hsieh CH (2001) Three-dimensional mapping of brain neuropils in the cockroach Diploptera punctata. J Comp Neurol 440(1):1–11. https://doi.org/10.1002/cne.1365
29. Fu YY, Lin CW, Enikolopov G, Sibley E, Chiang AS, Tang SC (2009) Microtome-free 3-dimensional confocal imaging method for visualization of mouse intenstine with subcellular-level resolution. Gastroenterologia 137(2):453–465. https://doi.org/10.1053/j.gastro.2009.05.008
30. Liu YC, Chiang AS (2003) High-resolution confocal imaging and three-dimensional rendering. Methods 30(1):86–93. https://doi.org/10.1016/S1046-2023(03)00010-0
31. Hara M, Noiseux N, Bindokas V (2005) High resolution optical imaging of infarction in intact organs. BioTechniques 39(3):373–376. PMID: 16206909. https://www.ncbi.nlm.nih.gov/pubmed/16206909
32. Tsien RY (1998) The green fluorescent protein. Annu Rev Biochem 67:509–544. https://doi.org/10.1146/annurev.biochem.67.1.509
33. Ward W (2005) Biochemical and physical properties of green fluorescent protein. In: Chalfie M, Kain SR (eds) Green fluorescent protein, 2nd edn. Wiley Interscience, New York, pp 39–65
34. Saghafi S, Becker K, Jährling N, Hahn C, Dodt H-U (2020) Ultramicroscopy of nerve fibers and neurons: fine-tuning the light sheets. In: Pelc R, Walz W, Doucette JR (eds) Neurohistology and imaging techniques, Neuromethods, vol 153. Springer (Humana Press), New York, pp 325–339. https://doi.org/10.1007/978-1-0716-0428-1_11
35. Burdock GA, Ford RA (1992) Safety evaluation of dibenzyl ether. Food Chem Toxicol 30(7):559–566. https://doi.org/10.1016/0278-6915(92)90189-R
36. Eichel FG, Othmer DF (1949) Bezaldehyde by autoxidation of dibenzyl ether. Ind Eng Chem 41(11):2623–2626. https://doi.org/10.1021/ie50479a054
37. Dasler W, Bauer CD (1946) Removal of peroxides from organic solvents. Ind Eng Chem Anal Ed 18(1):52–54. (incorporated into Anal Chem). https://doi.org/10.1021/i560149a017
38. Brady OL, Elsmie GV (1926) The use of 2,4-dinitrophenylhydrazine as a reagent for aldehydes and ketones. Analyst 51:77–78. https://doi.org/10.1039/AN9265100077
39. Mufson EJ, Perez SE, Kelley CM, Alldred MJ, Ginsberg SD (2020) Fixation protocols for neurohistology: neurons to genes. In: Pelc R, Walz W, Doucette JR (eds) Neurohistology and imaging techniques, Neuromethods, vol 153. Springer (Humana Press), New York, pp 49–71. https://doi.org/10.1007/978-1-0716-0428-1_2
40. Feng G, Mellor RH, Bernstein M, Keller-Peck C, Nguyen QT, Wallace M, Nerbonne JM, Lichtman JW, Sanes JR (2000) Imaging neuronal subsets in transgenic mice expressing multiple spectral variants of GFP. Neuron 28(1):41–51. https://doi.org/10.1016/S0896-6273(00)00084-2

NEUROMETHODS

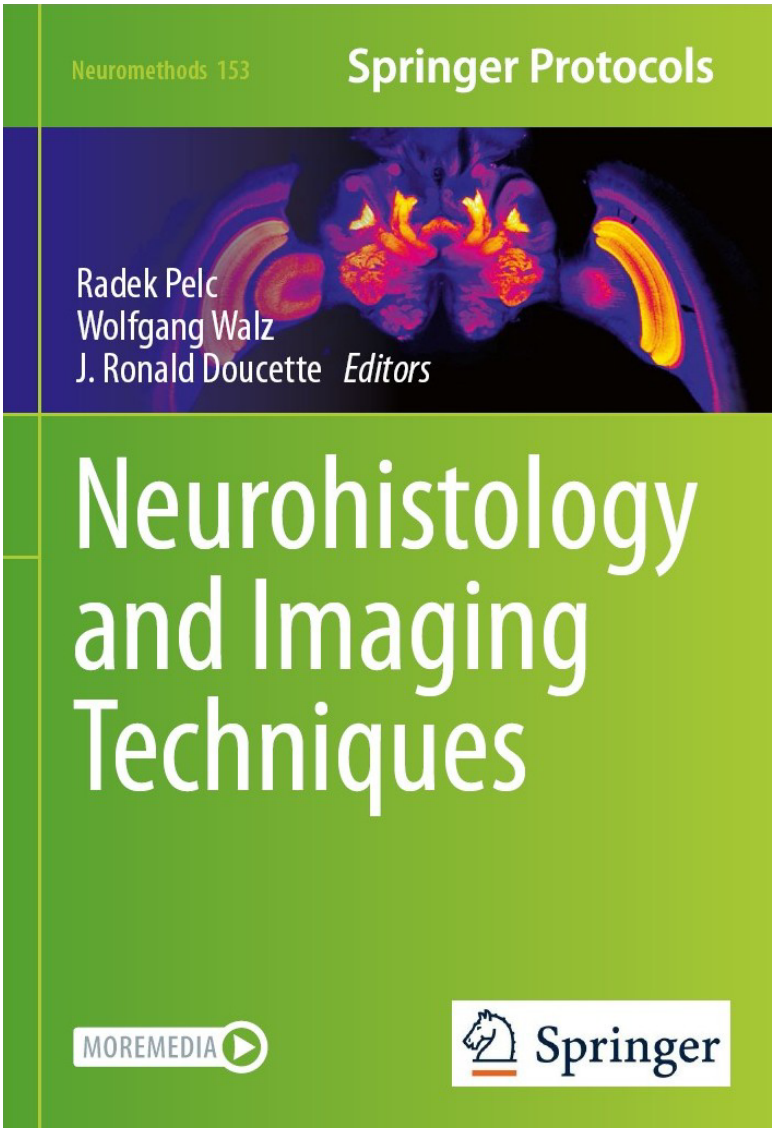

For further volumes:
http://www.springer.com/series/7657